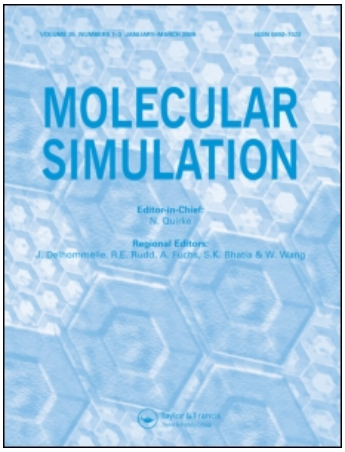

Molecular Simulation
Publication details, including instructions for authors and subscription information:
http://www.informaworld.com/smpp/title~content=t713644482

Molecular dynamics simulation on the decomposition of type SII hydrogen hydrate and the performance of tetrahydrofuran as a stabiliser

Chun-Yu Geng[ab]; Qing-Zhen Han[a]; Hao Wen[a]; Zhen-Yu Dai[c]; Chun-Hua Song[d]
[a] State Key Laboratory of Multi-Phase Complex System, Institute of Process Engineering, Chinese Academy of Sciences, Beijing, P.R. China [b] Graduate University of Chinese Academy of Sciences, Beijing, P.R. China [c] Research Institute of Petroleum Processing, SINOPEC, Beijing, P.R. China [d] Marine College, Shandong University at Weihai, Weihai, P.R. China

Online publication date: 11 May 2010

To cite this Article Geng, Chun-Yu , Han, Qing-Zhen , Wen, Hao , Dai, Zhen-Yu and Song, Chun-Hua(2010) 'Molecular dynamics simulation on the decomposition of type SII hydrogen hydrate and the performance of tetrahydrofuran as a stabiliser', Molecular Simulation, 36: 6, 474 — 483
To link to this Article: DOI: 10.1080/08927021003664041
URL: http://dx.doi.org/10.1080/08927021003664041

Molecular Simulation
Vol. 36, No. 6, May 2010, 474–483

Taylor & Francis
Taylor & Francis Group

Molecular dynamics simulation on the decomposition of type SII hydrogen hydrate and the performance of tetrahydrofuran as a stabiliser

Chun-Yu Geng[ab], Qing-Zhen Han[a], Hao Wen[a]*, Zhen-Yu Dai[c] and Chun-Hua Song[d]

[a]*State Key Laboratory of Multi-Phase Complex System, Institute of Process Engineering, Chinese Academy of Sciences, No. 1, 2nd North Lane, ZhongGuanCun, Beijing 100190, P.R. China;* [b]*Graduate University of Chinese Academy of Sciences, P.O. Box 4588, Beijing 100049, P.R. China;* [c]*Research Institute of Petroleum Processing, SINOPEC, No. 18, Xueyuan Road, Beijing 100083, P.R. China;* [d]*Marine College, Shandong University at Weihai, No. 180, Wenhua West Road, Weihai 264209, P.R. China*

(*Received 8 October 2009; final version received 30 January 2010*)

Molecular dynamics simulation is used to study the decomposition and stability of SII hydrogen and hydrogen/tetrahydrofuran (THF) hydrates at 150 K, 220 K and 100 bar. The modelling of the microscopic decomposition process of hydrogen hydrate indicates that the decomposition of hydrogen hydrate is led by the diffusive behaviour of H_2 molecules. The hydrogen/THF hydrate presents higher stability, by comparing the distributions of the tetrahedral angle of H_2O molecules, radial distribution functions of H_2O molecules and mean square displacements or diffusion coefficients of H_2O and H_2 molecules in hydrogen hydrate with those in hydrogen/THF hydrate. It is also found that the resistance of the diffusion behaviour of H_2O and H_2 molecules can be enhanced by encaging THF molecules in the ($5^{12}6^4$) cavities. Additionally, the motion of THF molecules is restricted due to its high interaction energy barrier. Accordingly, THF, as a stabiliser, is helpful in increasing the stability of hydrogen hydrate.

Keywords: gas hydrate; molecular dynamics; stability; decomposition; clathrate

1. Introduction

Gas hydrates are a class of inclusion compounds in which gas molecules, fully or partially, occupy cavities in the host framework made up of hydrogen-bonded water molecules [1]. The research of natural gas hydrate (NGH), being the most attractive gas hydrate, is of fundamental and practical importance for its abundant reserve buried in the permafrost and sediments underneath the continental shelf [2]. NGH is also expected to become a new medium for energy storage and transportation because of its stability below 273 K at atmospheric pressure [3].

The synthesis of hydrogen hydrate, a hydrate of H_2 molecules with multiple occupancies at extremely high pressure and low temperature, questioned the conventional theory for the prediction of the stability of clathrate hydrate [4]. Florusse et al. [5] have reported that hydrogen hydrate can be stabilised and stored at much lower pressures within a clathrate hydrate lattice by stabilising large cavities with a second guest component, tetrahydrofuran (THF). They have also revealed that the hydrogen/THF hydrate has a crystal structure of type SII by X-ray diffraction measurement. In addition, Lee et al. [6] have found that the storage of hydrogen in THF-containing binary clathrate hydrates can get to 4 wt%, and THF molecules will occupy the large cavities completely when the THF mole fraction is higher than 0.020. Hashimoto et al. [7] have measured the phase equilibria of the H_2/THF/H_2O ternary mixture at various THF concentrations. Investigating the effect of THF in hydrogen hydrate, Alavi et al. [8] have found that the THF molecules have a stabilising effect on the lattice energy, and the configurational energy of the unit cell will decrease upon addition of more THF molecules in the large cavities by molecular dynamics (MD) simulations. The performance of THF in stabilising the hydrogen hydrates raises the prospect of using clathrate hydrate as a new medium for hydrogen storage and transportation.

In this paper, the decomposition process of type SII hydrogen hydrate is investigated using MD. The stability of SII hydrogen hydrate and the performance of THF as a stabiliser are discussed at the molecular level.

2. Simulation details

A unit cell of type SII gas hydrate is composed of 16 small and 8 large cavities. The small cavity, a dodecahedral framework of 12 pentagons, is composed of 20 H_2O molecules, and is represented as (5^{12}) in this work for simplification, while the large cavity, a hexadecahedral framework of 12 pentagons and 4 hexagons, is composed of 28 H_2O molecules and represented as ($5^{12}6^4$). For a fully occupied hydrogen hydrate, according to the results of Patchkovskii and Tse [9], two H_2 molecules are encaged in each (5^{12}) cavity, and four H_2 molecules in each ($5^{12}6^4$)

*Corresponding author. Email: hwen@home.ipe.ac.cn

ISSN 0892-7022 print/ISSN 1029-0435 online

DOI: 10.1080/08927021003664041
http://www.informaworld.com

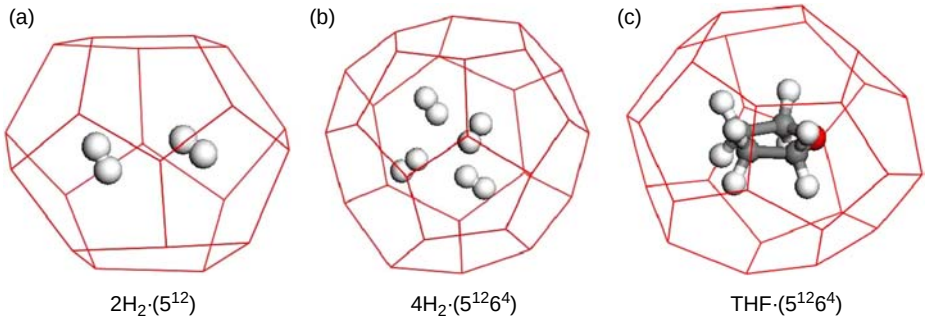

Figure 1. Schematic framework of H_2O molecule cavities occupied by H_2 and THF molecules in type SII gas hydrates. Encaged colour scheme: red for O atoms, light grey for H atoms and dark grey for C atoms (colour online).

cavity, represented as $2H_2\cdot(5^{12})$ and $4H_2\cdot(5^{12}6^4)$. For hydrogen/THF hydrate, each $(5^{12}6^4)$ cavity is assumed to be occupied by a THF molecule instead of four H_2 molecules, represented as $THF\cdot(5^{12}6^4)$. The (5^{12}) and $(5^{12}6^4)$ cavities with encaged H_2 and THF molecules are shown in Figure 1.

The thermodynamic stability results of Patchkovskii and Tse [9] have confirmed the multiple occupancy of clathrate cavities with average occupations of 2.00 and 3.96 H_2 molecules in small and large cavities, respectively, although the most stable configurations can sometimes have single occupancy in small cavities and quadruple occupancy in large cavities at some conditions [10]. Therefore, the fully occupied type of SII hydrogen hydrate, constructed by H_2 molecule-occupied cavities, $2H_2\cdot(5^{12})$ and $4H_2\cdot(5^{12}6^4)$, is taken as the model system of hydrogen hydrate in this work. The model system of hydrogen/THF hydrate is constructed by H_2 and THF molecule-occupied cavities, $2H_2\cdot(5^{12})$ and $THF\cdot(5^{12}6^4)$. The model systems are prepared in a simulation box of a $2 \times 2 \times 2$ unit cell with periodic boundary conditions, as shown in Figure 2. The initial positions of H_2O molecules in the model systems are taken from the X-ray diffraction measurements [11,12]. Additionally, all the atomic positions are allowed to freely translate during the simulation.

The *NPT* ensemble MD simulations are performed with the CVFF force field at temperature $T = 150$ K, 220 K and pressure $P = 100$ bar, using the Materials Studio software [13]. The system temperature and pressure are controlled using the Andersen [14] and Berendsen [15] methods. The initial equilibrations of the model systems are optimised by both steepest-descent and conjugate gradient methods. The van der Waals and long-range Coulomb interactions are calculated using the Ewald summation. The Verlet-velocity algorithm [16] is used to obtain accurate integrations and statistical ensembles.

A simulation time of 200 ps with an integration time step of 1 fs is typically employed, and simulations of the first 50 ps are used for equilibration. All the simulations are performed on the server with Intel Xeon CPU E5335 2.0 GHz and 4 G memory.

The interaction energy ΔE is calculated, in order to estimate the stability of hydrogen-bonded water cavities occupied by different guest molecules, following the definition presented in Equation (1):

$$\Delta E = E_{\text{GH-cavity}} - E_{\text{H-cavity}} - E_{\text{gas}}, \tag{1}$$

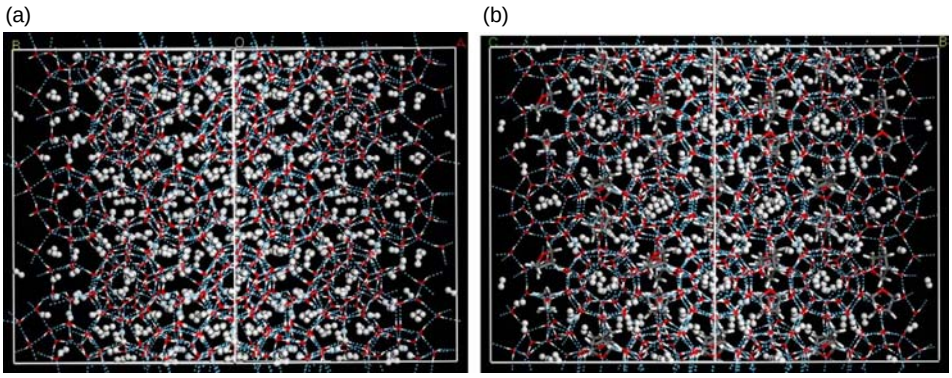

Figure 2. The model systems of $2 \times 2 \times 2$ fully occupied type SII hydrogen and hydrogen/THF hydrates.

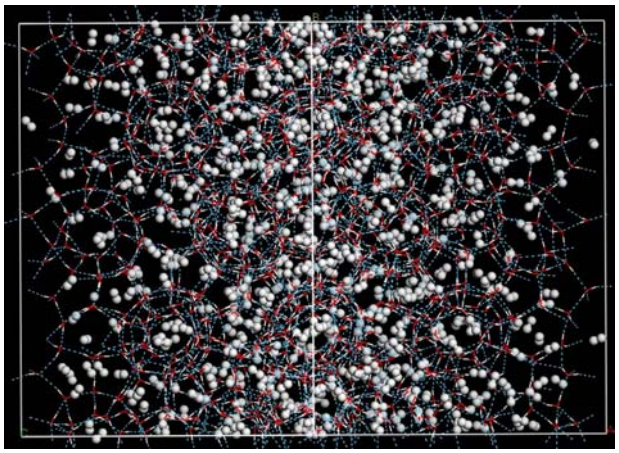

Figure 3. The final snapshot of hydrogen hydrate at $T = 150$ K and $P = 100$ bar.

where $E_{\text{GH-cavity}}$, $E_{\text{H-cavity}}$ and E_{gas} denote the total energies of the encaged gas molecule cavity, hydrogen-bonded water cavity and gas molecule, respectively.

The energy calculations are performed by the semi-empirical method PM3 and VSTO-3G (5D, 7F) basis set in the Gaussian03 program [17] on the Shenteng 6800 workstation referred by the Computer Network Information Center (CNIC), Chinese Academy of Sciences.

3. Results and discussion

3.1 Decomposition of hydrogen hydrate

The final configuration of hydrogen hydrate at 150 K and 100 bar is shown in Figure 3. It can be seen from Figure 3 that the crystalline structure of hydrogen hydrate can keep stable at $T = 150$ K.

The radial distribution functions (RDFs) of O atoms in H_2O molecules, $g_{OO}(r)$, within the simulation run time intervals $t = 50–100$ and 150–200 ps at 150 K and 100 bar are presented in Figure 4. The RDF is defined as the probability of finding an identical atom at a distance r apart from another. For a stable type SII hydrate, there exist two distinct peaks in the RDF of O atoms. The maximal RDF peak of O atoms appears at a distance $r_{OO} = 2.78$ Å, corresponding to the nearest distance of O atoms between neighbouring H_2O molecules separated from each other at around 2.78 Å. The second maximal peak appeared at $r_{OO} = 4.53$ Å, indicating the existence of tetrahedral hydrogen bonding structures of H_2O molecules in hydrogen hydrates. In the case of liquid water, where the tetrahedral hydrogen bonding structures of H_2O molecules are destroyed, the second maximum RDF peak is almost horizontal [18]. While in Figure 4, it is apparent that the RDF peaks of O atoms at $t = 50–100$ and 150–200 ps are almost similar, which indicates that the structure of hydrogen hydrate can keep stable at $T = 150$ K.

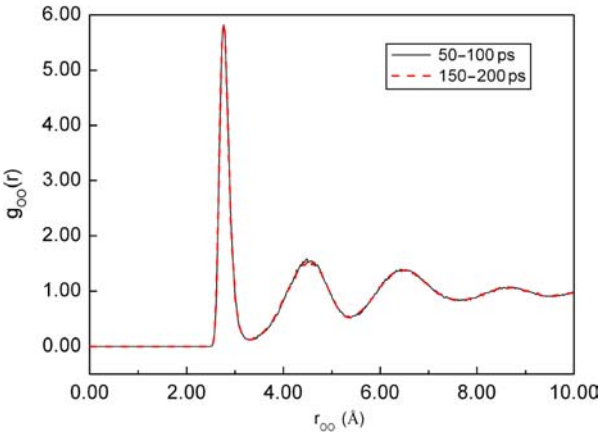

Figure 4. RDFs of O atoms in H_2O for hydrogen hydrate at 150 K within the run time intervals $t = 50–100$ and 150–200 ps.

The mean square displacements (MSDs) of H_2O and H_2 molecules within the run time interval $t = 50–100$ ps at 150 K and 100 bar are depicted in Figure 5. The MSD as a function of time is a measure of the average distance a molecule travels over the time interval and can be used to represent the amplitude of the thermal vibration of a molecule, which is defined as

$$R(t') = \frac{1}{N}\sum_{i=1}^{N}\left\langle \left[R_i(t_0 + t') - R_i(t_0)\right]^2 \right\rangle, \qquad (2)$$

where t_0 is the reference time; $R(t')$ is the MSD over the run time interval t'; $R_i(t_0)$ and $R_i(t_0 + t')$ are, respectively, the positions of molecule i at run times t_0 and $t_0 + t'$; and the summation is over all the finite systems containing N identical molecules.

Figure 5 indicates that, at low temperature $T = 150$ K, the MSD profile of water molecules is typical of a stable crystal, while H_2 molecules are continuously moving in the hydrate cavities.

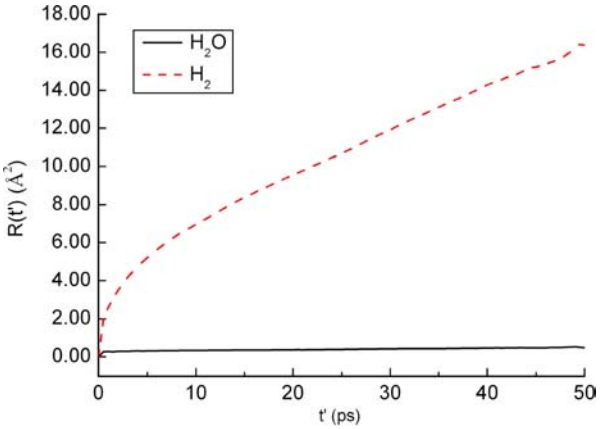

Figure 5. MSDs of H_2 and H_2O molecules at $T = 150$ K and $P = 100$ bar.

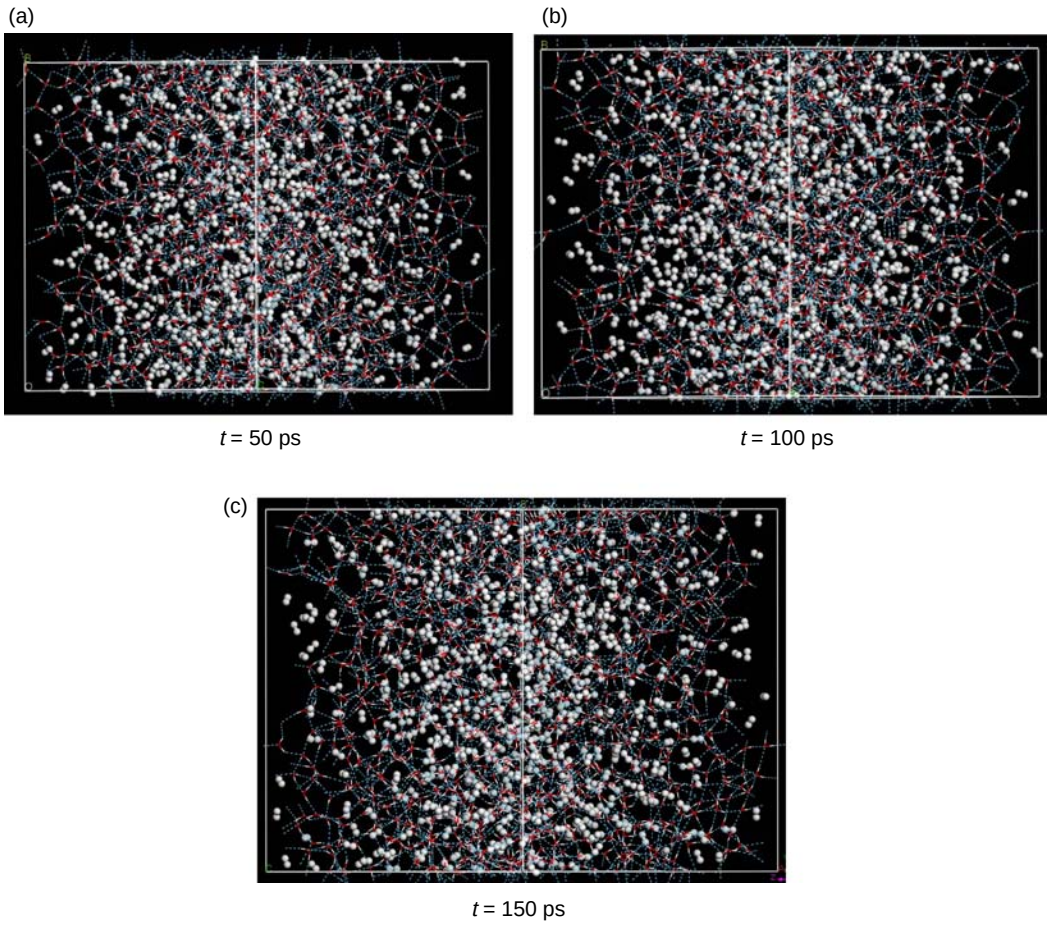

Figure 6. Snapshots of the decomposition process of hydrogen hydrate at $T = 220$ K and $P = 100$ bar.

The microscopic decomposition process of hydrogen hydrate at 220 K and 100 bar is presented in Figure 6, the configuration snapshots of which are taken at simulation run times $t = 50$, 100 and 150 ps. Comparing the initial and final configurations, Figure 6 shows that the cavities of hydrogen hydrate will be gradually destroyed with the simulation time running. An evident molecular aggregation of H_2 molecules can be observed when the simulation run time $t > 150$ ps.

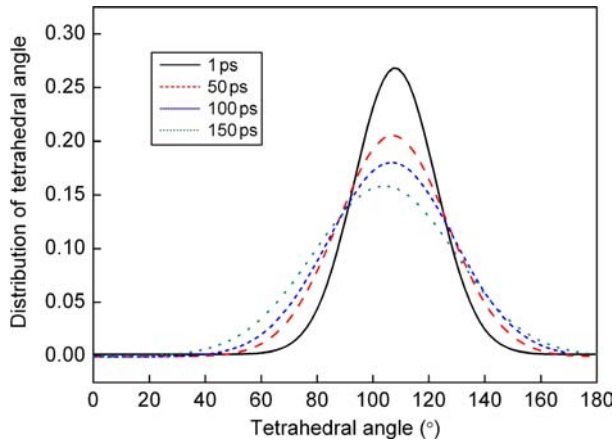

Figure 7. Distribution of tetrahedral angles of H_2O molecules in hydrogen hydrate at $T = 220$ K and $P = 100$ bar.

Correspondingly, Figure 7 presents the distributions of the tetrahedral angle of H_2O molecules in hydrogen hydrate at simulation run times $t = 50$, 100 and 150 ps, for investigating the change in the hydrogen-bonded network during hydrogen hydrate decomposition at 220 K and 100 bar. In a stable hydrate, each H_2O molecule will hydrogen bond with four H_2O molecules and form a tetrahedral hydrogen-bonded network. The tetrahedral angle of H_2O molecules is thus defined as the average bond angle formed by the central O atom with pairs of O atoms from its neighbouring hydrogen-bonded H_2O molecules, which is close to 109.47°, and can be seen as a probe of the stability of hydrogen-bonded network. Obviously, the distribution of the tetrahedral angle for H_2O molecules in Figure 7 gradually weakens and broadens with the run time increasing, which indicates that the cavities of hydrogen hydrate will gradually destroy with the simulation time running.

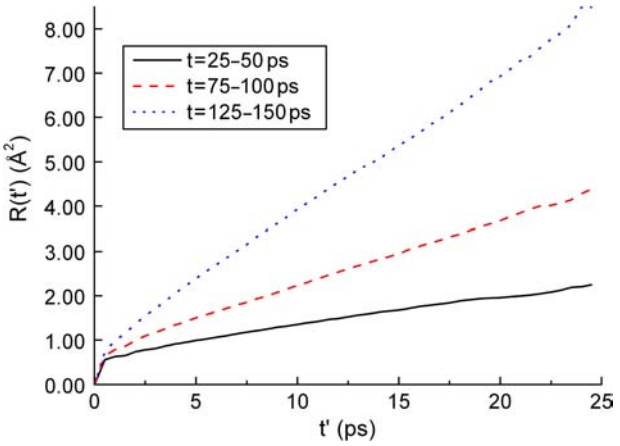

Figure 8. MSDs of H_2O molecules at run time intervals $t = 25–50$, 75–100 and 125–150 ps.

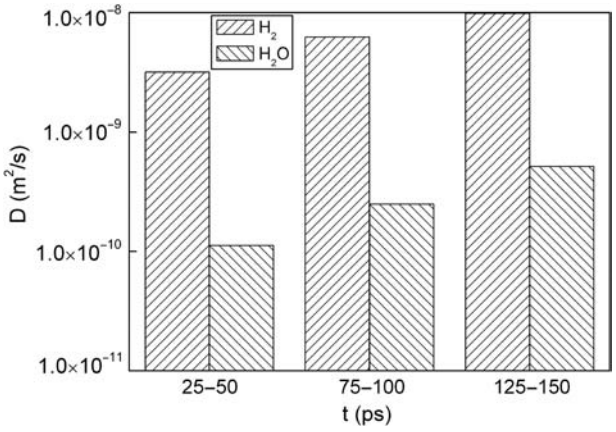

Figure 9. Diffusion coefficients of H_2 and H_2O molecules within the run time intervals $t = 25–50$, 75–100 and 125–150 ps.

The MSDs of H_2O molecules at 220 K and 100 bar within the run time intervals $t = 25–50$, 75–100 and 125–150 ps are depicted in Figure 8. Within the run time interval $t = 25–50$ ps, the MSD of H_2O molecules is slightly diffusive, although the configuration can keep a regular hydrogen-bonded network, as shown in Figure 6(a). As the crystal distortion becomes more pronounced within the run time interval $t = 75–100$ ps, the MSD of H_2O molecules also becomes a little larger. Within the run time interval $t = 125–150$ ps, the MSD of H_2O molecules is much higher than those within $t = 25–50$ and 75–100 ps, which indicates that H_2O molecules are continually diffusing with time running.

Figure 9 displays the diffusion coefficients of H_2O and H_2 molecules within the run time intervals $t = 25–50$, 75–100 and 125–150 ps at 220 K and 100 bar. The diffusion coefficient can be obtained from the Einstein relation

$$6Dt' = \langle R(t') \rangle, \tag{3}$$

where D is the diffusion coefficient and $R(t')$ is the MSD within the time interval t'. The diffusion coefficient of H_2 molecules indicates that H_2 molecules are continuously moving in the hydrate cavities, whereas the hydrate lattice is not destroyed. The calculated diffusion coefficient of H_2 molecules is much higher than that of H_2O molecules all the time, which also indicates that the movement of H_2 molecules will be more violent than that of H_2O molecules.

The RDFs of O atoms in H_2O molecules, $g_{OO}(r)$, within the simulation run time intervals $t = 25–50$, 75–100 and 125–150 ps at 220 K and 100 bar are presented in Figure 10. In Figure 10, the second maximal RDF peak becomes lower and broader with the simulation time running, which indicates the reduction of tetrahedral hydrogen bonding structures of H_2O molecules or the loss of hydrate stability at 220 K and 100 bar.

Figure 11 shows that the cell size of hydrogen hydrate will gradually increase during the decomposition process. Here, the cell size is the volume of the unit cell of hydrogen hydrate. Considering the diffusion of H_2O and H_2 molecules, the diffusion will be gradually higher with increasing run time, which results in a looser structure and severe corruption. The increase in cell size indicates that the crystal structure cannot keep stable and will be broken completely.

As a result, the decomposition of hydrogen hydrate is such a process that the gradually active movements of H_2O and H_2 molecules lead the H_2O molecules to depart from their lattice sites and H_2 molecules to diffuse from the cavities. The monotonous increasing of diffusion of H_2O and H_2 molecules exhibits the feature of hydrate crystal distortion and cell size increasing. The hydrate cavities

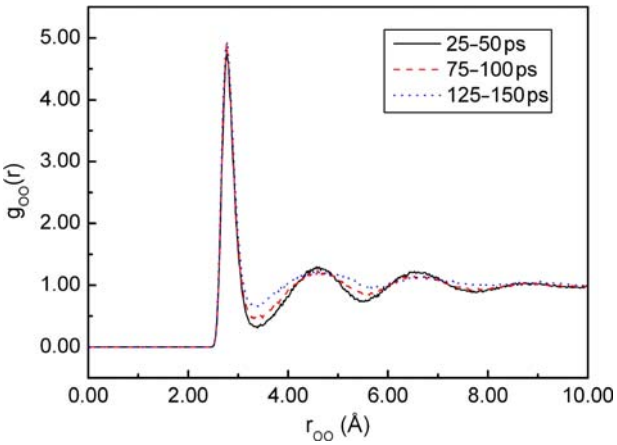

Figure 10. RDFs of O atoms in H_2O molecules for hydrogen hydrate within the run time intervals $t = 25–50$, 75–100 and 125–150 ps.

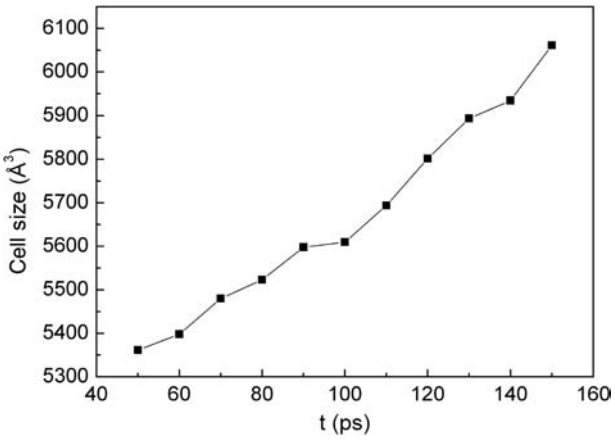

Figure 11. Cell size of hydrogen hydrate at $T = 220$ K and $P = 100$ bar within the run time interval $t = 50–150$ ps.

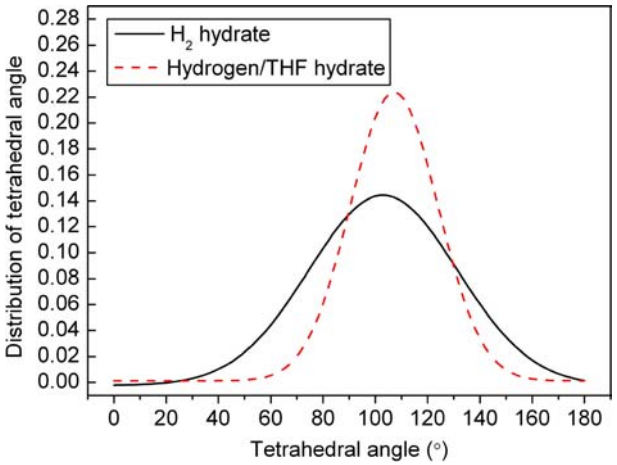

Figure 13. Distribution of tetrahedral angles of H_2O molecules in hydrogen and hydrogen/THF hydrates at $T = 220$ K and $P = 100$ bar.

will be destroyed when the distortion is too severe to maintain a stable lattice structure. It is obvious that, however, the diffusion of H_2 molecules is always much larger than that of H_2O molecules. This phenomenon is somewhat different from the decomposition of methane hydrate [19].

3.2 Stability of hydrogen hydrate and hydrogen/THF hydrate

The snapshots of final configurations of hydrogen and hydrogen/THF hydrates at temperature $T = 220$ K and pressure $P = 100$ bar are shown in Figure 12(a),(b), respectively. Figure 12(a) shows that the cavity framework of hydrogen hydrate has already collapsed compared with its initial configuration in Figure 2(a), and H_2 molecules exhibit an evident molecular aggregation. However, the cavity framework of hydrogen/THF hydrate can still keep stable, although the occurrence of some distortions can be observed.

As shown in Figure 13, the distribution of the tetrahedral angle of H_2O molecules in hydrogen hydrate is obviously lower and broader than that in hydrogen/THF hydrate. This phenomenon can also confirm that the cavity framework of hydrogen/THF hydrate is more stable than that of hydrogen hydrate.

The sharper RDF peaks of O atoms in H_2O molecules for hydrogen/THF hydrate also state that the cavity framework of hydrogen/THF hydrate is more stable than that of hydrogen hydrate at 220 K and 100 bar, as shown in Figure 14.

Figure 15 presents the MSDs of H_2O and H_2 molecules within the run time interval $t = 50–200$ ps in hydrogen and hydrogen/THF hydrates at temperature $T = 220$ K and pressure $P = 100$ bar. Both H_2O and H_2 molecules in hydrogen hydrate diffuse more actively than they do

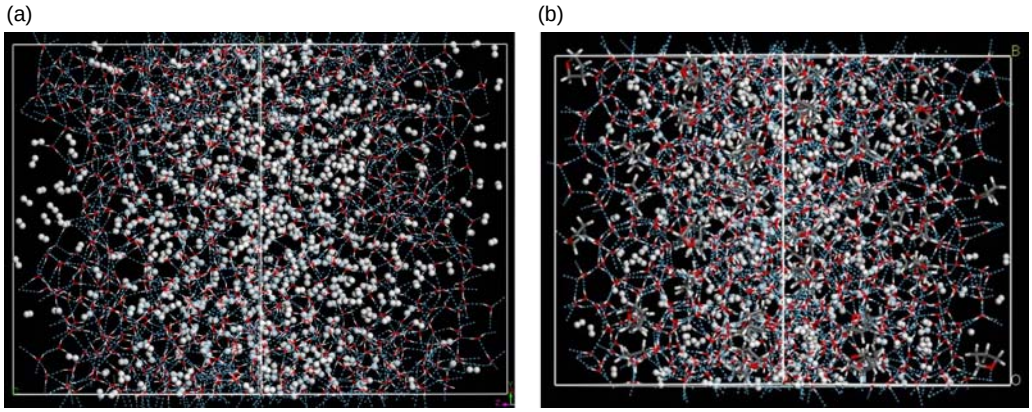

Figure 12. Snapshots of final configurations of hydrogen and hydrogen/THF hydrates at $T = 220$ K and $P = 100$ bar.

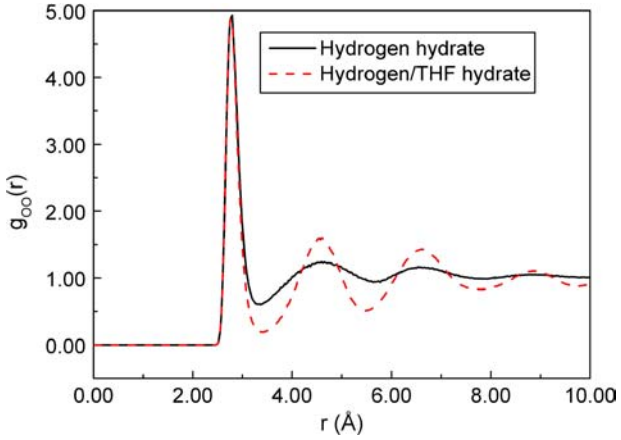

Figure 14. RDFs of O atoms in H_2O for hydrogen and hydrogen/THF hydrates at $T = 220$ K and $P = 100$ bar.

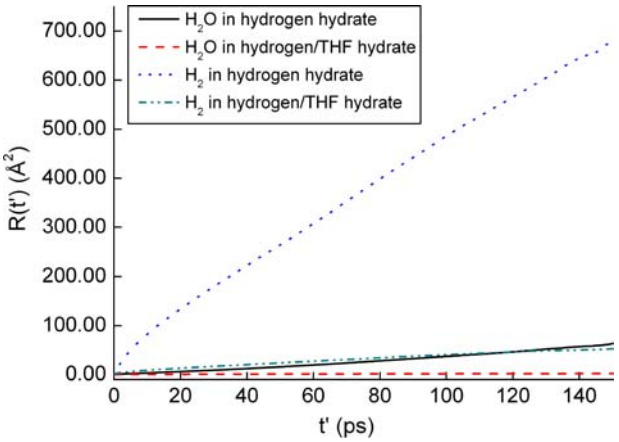

Figure 15. MSDs of H_2O and H_2 molecules in hydrogen and hydrogen/THF hydrates within the run time interval $t = 50$–200 ps.

in hydrogen/THF hydrate at the same temperature and pressure. Additionally, the cell size of hydrogen hydrate will increase continually, while that of hydrogen/THF hydrate will keep steady, as shown in Figure 16. That means the decomposition of hydrogen hydrate is much severer than that of hydrogen/THF hydrate.

3.3 *Interaction energy*

Ding et al. [19] have concluded by their MD simulation study on the decomposition of methane hydrate that the diffusive behaviour of the cavity host H_2O molecules leads to the fracture of the lattice structure. However, it may be inferred from our results that the collapse of the cavity in either hydrogen hydrate or hydrogen/THF hydrate is caused by the diffusion of H_2 molecules rather than H_2O molecules, because the MSD and diffusion coefficient values of H_2 molecules whether at 150 or 220 K are always larger than those of H_2O molecules, as presented in Figures 5, 9 and 15. This may imply that the decomposition of hydrogen hydrate is mainly caused by the diffusion of H_2 molecules in the hydrate cavities.

To discuss the difference in the decompositions of hydrogen hydrate and methane hydrate, interactions between the guest (H_2 or CH_4) molecules and the hydrate lattice cavities are calculated. For an optimised hydrate cavity, the interaction between H_2, or CH_4, molecules at different positions can be depicted by the interaction energy. The interaction energy of the guest molecule in the hydrate cavity can be calculated according to Equation (1), as shown in Figure 17, when the guest molecule places along the joint line of its equilibration position to the centre of the pentagon or hexagon of the cavity. The centre of the pentagon or hexagon of the cavity is taken as the geometrical zero point, in the interaction energy calculations, and the direction towards the inside of the cavity is negative.

Figure 18 shows the interaction energies of the guest (CH_4 and H_2) molecules in the hydrate cavities as a function of their position relative to the fixed hydrate cavities. It is obvious that the interaction between the gas molecule and the hydrate cavity will become gradually stronger, when the gas molecule moves closer to the pentagon or hexagon of the cavity. As compared with the H_2 and CH_4 molecules, the motion of CH_4 molecules is much more restricted due to the evident interaction energy barrier, while the motion of H_2 molecules in cavities, especially in the ($5^{12}6^4$) cavities, is not as restricted as in CH_4 molecules. The very low interaction energy of H_2 molecules in the hydrate cavity means that H_2 molecules can move across the ($5^{12}6^4$) cavities of hydrogen hydrate easily without destroying the cavity structure, correspondingly the diffusion coefficient of H_2 molecules is always larger than that of H_2O molecules in hydrogen hydrate, as presented in Figure 9. Because of the easy movement across the hydrate cavities, H_2 molecules can diffuse

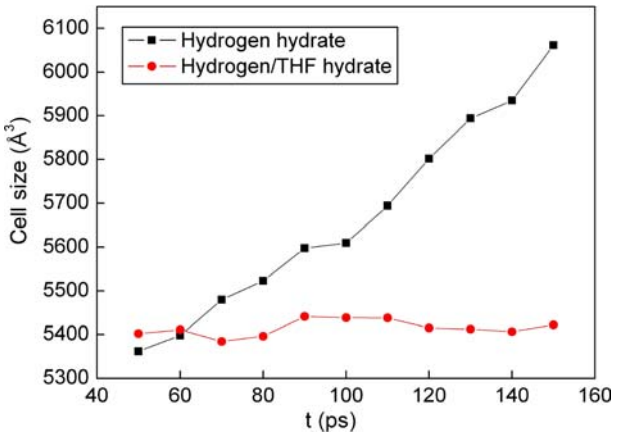

Figure 16. The cell size of hydrogen and hydrogen/THF hydrates within the run time interval $t = 50$–150 ps.

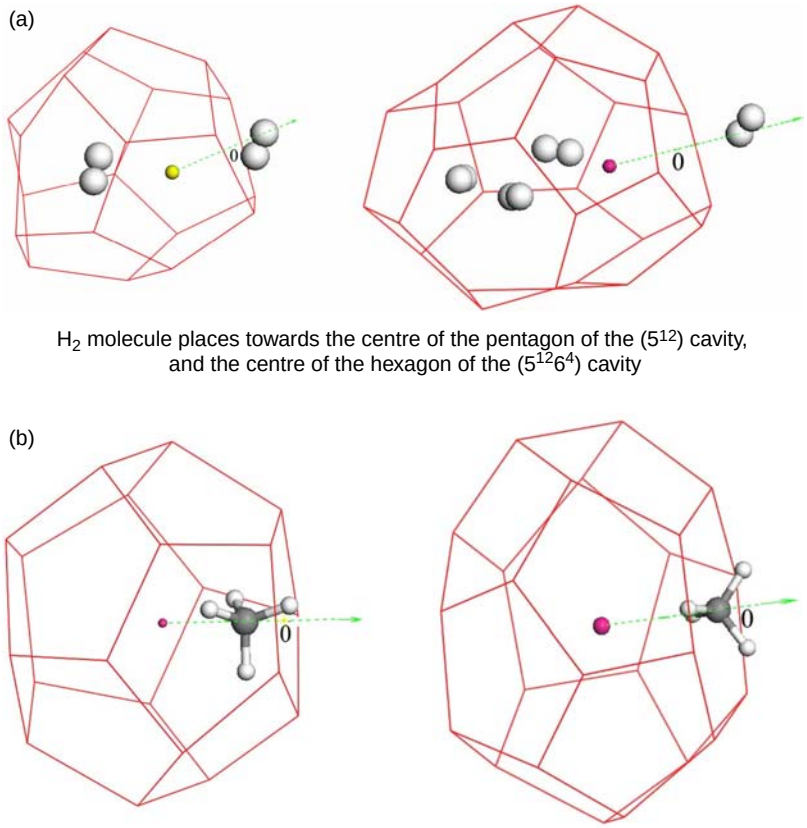

Figure 17. Schematic of H_2 and CH_4 molecules places along the joint line of the equilibration position to the centre of the pentagon or hexagon of the hydrate cavities.

outside and decrease the stability of the hydrate [10]. Accordingly, the decomposition process of hydrogen hydrate should be caused by the diffusion of H_2 molecules.

3.4 Performance of THF as a stabiliser

Compared with the stability of hydrogen and hydrogen/THF hydrates, hydrogen/THF hydrate exhibits higher stability when THF molecules occupy the large cavities. Alavi et al. [8] have investigated the configurational energies of different occupancy cases, and concluded that THF molecules have a stabilising effect on the clathrate and the configurational energy of the unit cell decreases linearly as the THF content increases.

Figure 19 presents the comparison of the interaction energies of H_2 and THF molecules in the ($5^{12}6^4$) cavities. The motion of THF molecules in the ($5^{12}6^4$) cavity will lead to a dramatic change in the interaction energy as compared with that of H_2 molecules. The high interaction energy barrier of THF molecules in the ($5^{12}6^4$) cavity makes sure that THF molecules cannot move easily unless the ($5^{12}6^4$) cavity is broken. This result is also represented in Figure 15 and shows that the MSD of H_2 molecules in hydrogen/THF hydrate is much lower than that in hydrogen hydrate, because of the existence of THF molecules. The motion of THF molecules in the hydrate cavity will be restricted by the high interaction energy barrier. The THF molecule is impossible to escape from the ($5^{12}6^4$) cavity unless cavity destroying happened. This makes the motion of H_2 molecules in hydrogen/THF hydrate to be much slower than it is in H_2 hydrate, because H_2 molecules cannot move to the ($5^{12}6^4$) cavities where the THF molecules are encaged in. The decomposition of hydrogen hydrate will be inhibited by the existence of THF molecules in the ($5^{12}6^4$) cavities of hydrogen/THF hydrate. Thus, performing as a stabiliser, THF molecules will enhance the stability of hydrogen hydrate, from either the interaction energy or diffusion point of view.

4. Conclusions

The *NPT* ensemble MD simulations are used to study the decomposition of type SII hydrogen hydrate, the stability

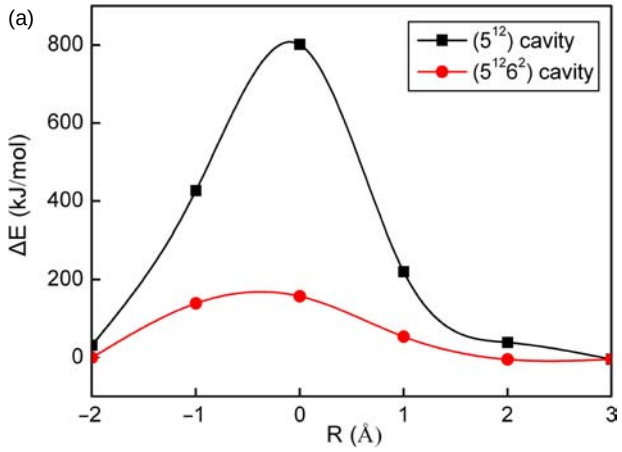

Figure 18. Interaction energies of CH_4 and H_2 molecules in hydrate cavities.

of hydrogen and hydrogen/THF hydrates, and the performance of THF as a stabiliser.

By modelling the microscopic decomposition of hydrogen hydrate, it is found that the diffusion of H_2 molecules is always larger than that of H_2O molecules, which is different from that of methane hydrate. That means the decomposition process of hydrogen hydrate is associated with the diffusive behaviour of H_2 molecules, which leads to the instability and the lattice destruction of hydrogen hydrate. The hydrogen/THF hydrate is more stable than hydrogen hydrate, with comparison of the distributions of the tetrahedral angle of H_2O molecules, RDFs of H_2O molecules, and MSDs or diffusion coefficients of H_2O and H_2 molecules in hydrogen and hydrogen/THF clusters.

The interaction energy between the guest molecules (CH_4, H_2 and THF) and hydrate lattice cavities explains how the decomposition of hydrogen hydrate differs from

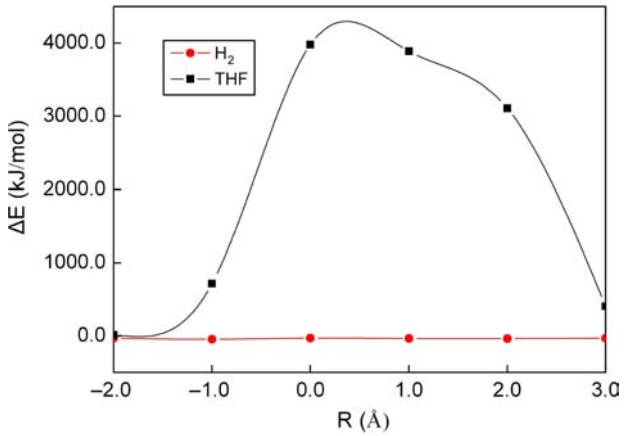

Figure 19. Interaction energy of H_2 and THF molecules in the ($5^{12}6^4$) cavity.

that of methane hydrate. Moreover, THF molecules encaged in the ($5^{12}6^4$) cavities perform as a stabiliser because of the high interaction energy barrier restricting the motion of THF molecules. THF can stabilise the hydrogen hydrate structures when THF is selected as a second guest component.

Acknowledgements

The authors gratefully appreciate the financial support from the Natural Science Foundation of China (No. 20821092). The authors also acknowledge the generous computational services provided by the Shenteng 6800 workstation referred by the Computer Network Information Center, Chinese Academy of Sciences.

References

[1] S. Subramanian and E.D. Sloan, Jr, *Trends in vibrational frequencies of guests trapped in clathrate hydrate cages*, J. Phys. Chem. B 106 (2002), pp. 4348–4355.
[2] E. Suess, G. Bohrmann, J. Greinert, and E. Lausch, *Flammable ice*, Sci. Am. 281 (1999), pp. 52–59.
[3] E.D. Sloan, Jr, *Clathrate Hydrates of Natural Gases*, 2nd ed., Marcel Dekker, New York, 1998.
[4] W.L. Mao, H.K. Mao, A.F. Goncharov, V.V. Struzhkin, Q. Guo, J. Hu, J. Shu, R.J. Hemley, M. Somayazulu, and Y. Zhao, *Hydrogen clusters in clathrate hydrate*, Science 297 (2002), pp. 2247–2249.
[5] J.L. Florusse, C.J. Peters, J. Schoonman, K.C. Hester, C.A. Koh, S.F. Dec, K.N. Marsh, and E.D. Sloan, Jr, *Stable low-pressure hydrogen clusters stored in a binary clathrate hydrate*, Science 306 (2004), pp. 469–471.
[6] H. Lee, J.W. Lee, D.Y. Kim, J. Park, Y.T. Seo, H.I. Zeng, L. Moudrakovski, C.I. Ratcliffe, and J.A. Ripmeester, *Tuning clathrate hydrates for hydrogen storage*, Nature 434 (2005), pp. 743–746.
[7] S. Hashimoto, T. Sugahara, H. Sato, and K. Ohgaki, *Thermodynamic stability of H_2 + tetrahydrofuran mixed gas hydrate in non-stoichiometric aqueous solutions*, J. Chem. Eng. Data 52 (2007), pp. 517–520.
[8] S. Alavi, J.A. Ripmeester, and D.D. Klug, *Molecular-dynamics simulations of binary structure II hydrogen*, J. Chem. Phys. 124 (2006), 014704.

[9] S. Patchkovskii and J.S. Tse, *Thermodynamic stability of hydrogen clathrate*, Proc. Natl Acad. Sci. USA 100 (2003), pp. 14645–14650.
[10] S. Alavi, J.A. Ripmeester, and D.D. Klug, *Molecular-dynamics study of structure II hydrogen clathrates*, J. Chem. Phys. 123 (2005), 024507.
[11] M.T. Kirchner, R. Boese, W.E. Billups, and L.R. Norman, *Gas hydrate single-crystal structure analyses*, J. Am. Chem. Soc. 126 (2004), pp. 9407–9412.
[12] K.A. Udachin, C.I. Ratcliffe, and J.A. Ripmeester, *Single crystal diffraction studies of structure I, II and H hydrates: Structure, cage occupancy and composition*, J. Supramol. Chem. 2 (2002), pp. 405–408.
[13] *Materials Studio, Version 4.0*. Accelrys Software, Inc., San Diego, CA, 2006.
[14] H.C. Andersen, *Molecular dynamics simulations at constant pressure and/or temperature*, J. Chem. Phys. 72 (1980), pp. 2384–2393.
[15] H.J.C. Berendsen, J.P.M. Postma, W.F. van Gunsteren, A. DiNola, and J.R. Haak, *Molecular dynamics with coupling to an external bath*, J. Chem. Phys. 81 (1984), pp. 3684–3690.
[16] L. Verlet, *Computer experiments on classical fluids. I. Thermodynamical properties of Lennard-Jones molecules*, Phys. Rev. 159 (1967), pp. 98–103.
[17] M.J. Frisch, G.W. Trucks, H.B. Schlegel, G.E. Scuseria, M.A. Robb, J.R. Cheeseman, J.A. Montgomery, Jr, T. Vreven, K.N. Kudin, J.C. Burant, J.M. Millam, S.S. Iyengar, J. Tomasi, V. Barone, B. Mennucci, M. Cossi, G. Scalmani, N. Rega, G.A. Petersson, H. Nakatsuji, M. Hada, M. Ehara, K. Toyota, R. Fukuda, J. Hasegawa, M. Ishida, T. Nakajima, Y. Honda, O. Kitao, H. Nakai, M. Klene, X. Li, J.E. Knox, H.P. Hratchian, J.B. Cross, C. Adamo, J. Jaramillo, R. Gomperts, R.E. Stratmann, O. Yazyev, A.J. Austin, R. Cammi, C. Pomelli, J.W. Ochterski, P.Y. Ayala, K. Morokuma, G.A. Voth, P. Salvador, J.J. Dannenberg, V.G. Zakrzewski, S. Dapprich, A.D. Daniels, M.C. Strain, O. Farkas, D.K. Malick, A.D. Rabuck, K. Raghavachari, J.B. Foresman, J.V. Ortiz, Q. Cui, A.G. Baboul, S. Clifford, J. Cioslowski, B.B. Stefanov, G. Liu, A. Liashenko, P. Piskorz, I. Komaromi, R.L. Martin, D.J. Fox, T. Keith, M.A. Al-Laham, C.Y. Peng, A. Nanayakkara, M. Challacombe, P.M.W. Gill, B. Johnson, W. Chen, M.W. Wong, C. Gonzalez, and J.A. Pople, *Gaussian 03, Revision C.02*, Gaussian, Wallingford, CT, 2004.
[18] L.Y. Ding, C.Y. Geng, Y.H. Zhao, X.F. He, and H. Wen, *Molecular dynamics simulation for surface melting and self-preservation effect of methane hydrate*, Sci. China Ser. B Chem. 51 (2008), pp. 651–660.
[19] L.Y. Ding, C.Y. Geng, Y.H. Zhao, and H. Wen, *Molecular dynamics simulation on the dissociation process of methane hydrates*, Mol. Simul. 33 (2007), pp. 1005–1016.